N. Sreenivasan
Centre for Advanced Materials Joining,
University of Waterloo,
Waterloo, ON, N2K 4K8, Canada

M. Xia
Centre for Advanced Materials Joining,
University of Waterloo,
Waterloo, ON, N2K 4K8, Canada;
Central Iron and Steel Research Institute,
Beijing 100081, P.R.C.

S. Lawson

Y. Zhou

Centre for Advanced Materials Joining,
University of Waterloo,
Waterloo, ON, N2K 4K8, Canada

Effect of Laser Welding on Formability of DP980 steel

Limiting dome height (LDH) tests were used to evaluate the formability of laser butt welded blanks of the dual phase 980 steel in comparison with the base metal. Two different lasers were used: diode and Nd:YAG, giving a wide range of welding thermal cycles. A sharp decrease in LDH was observed in the welded specimens due to the formation of a softened zone in the outer heat affected zone. Softened zone characteristics were correlated with the LDH. Larger softened zones led to a larger reduction in the LDH. The welding orientation relative to the rolling direction or to the punch surface did not influence the formability, as the softened zone dominated the formability behavior. It was observed that in both uniaxial and biaxial strain tests, the fracture occurred in the softened zone of the welded samples consistently slightly farther out from the weld centerline than in the location of the minimum hardness. [DOI: 10.1115/1.2969246]

Keywords: diode laser, Nd:YAG laser, formability, DP980 steel, softened HAZ

1 Introduction

Currently, many new types of advanced high strength steels (AHSSs), including dual phase (DP) steels, are being produced by steel manufacturers that have higher strength and ductility, which contribute to weight reduction in the automotive industries.

Most of the early weldability research on DP steels was focused on the resistance spot weld (RSW) technique [1,2]. Recent research has dealt with laser welding of DP steels with focus on the process development and optimization of the laser welding process [3–5]. Most commonly used lasers for welding are CO_2 and Nd:YAG [6–8]; however, the high power diode laser (HPDL) has also been confirmed to be well suited for welding of butt and lap-fillet joint geometries in the aluminum sheet for automotive applications as well as for butt welds in the steel [9–11].

Formability aspects of these steels and tailor welded blanks (TWBs) are also of interest and have been studied. Numerous studies have confirmed that in formability experiments of TWB, strain is concentrated and fracture occurs in the thinner/weaker side of the blank [12–15]. Further research has also suggested that the welding and rolling direction of the material may influence the formability [8,16]. On the other hand, it is known that laser welds in AHSS are harder/stronger than the base metal [17], and the surrounding heat affected zone (HAZ) contains regions that may be harder or softer [17]. Therefore, some significant effects of welding on formability would be expected.

The softened HAZ phenomenon has been observed in DP steels with various welding processes such as arc, RSW, and laser [5]. The softened HAZ in the arc and resistance welded DP steels had a significant influence on the formability [5]. Laser welding created a narrower softened zone with higher laser power and welding speed (6 kW, 7 m/min), in contrast to a wider softened zone created with lower power and speed (3 kW, 4 m/min) [18].

An introductory study on the influence of welding phenomena on the formability of high strength low alloy (HSLA) and DP980 steels was conducted at the authors' laboratory [19]. It was found that formability was not affected by the laser welding process on the HSLA material, whereas a decrease in formability was observed on the DP980 steel. Uniaxial transverse tensile testing of DP980 also showed a sharp decrease in maximum strain after welding. Furthermore, the influence of softened outer HAZs of the welds of the DP980 steel on the formability was observed.

This study focuses on the formability effects of the welds made with two different power density types of laser on the DP 980 steel, spanning a wide range of welding thermal cycles. The influence of the softened zone on formability is examined. The effect of the welding speed on fracture and softened zone distances from the weld centerline is studied. Furthermore, the relationship between uniaxial and biaxial strains is examined.

2 Experimental Procedures

2.1 Material. The DP 980 steel of 1.17 mm thickness with a coating described as galvannealed (GA) 48–55 g/m^2 with about 10% Fe was used in this study. The chemical and mechanical properties are summarized in Tables 1 and 2. Since the full chemical composition of the steel was considered proprietary, a summary of the alloying is provided including carbon equivalent using the well known Yurioka formula [20]. This DP steel has a ferrite matrix with a significant volume fraction of fine martensite laths.

2.2 Laser Properties. Diode and Nd:YAG are the two lasers used in this work and their characteristics are shown in Table 3. The Nuvonyx 4 kW diode laser was mounted on the manipulator arm of a welding robot. Its laser beam is rectangular in shape, with dimensions 12×0.5 mm^2 at the focal point. The energy density/irradiance of the diode laser, which is less than 10^6 W/cm^2, generates only a conduction mode of laser welding [21,22]. Ultrahigh purity argon gas was supplied at a flow rate of 14 l/min as a shielding gas at the leading edge of the laser beam spot on the top surface side of the welds. Welds were conducted in the bead on a plate mode, i.e., a butt weld with full penetration on the blanks of uniform thickness and material. Welding was conducted on the blanks within the speed range of 0.7–1.9 m/min. The welding speed of less than 0.7 m/min led to excess weld size and sag; the speed above 1.9 m/min resulted in partial penetration.

The Haas HL3006D Nd:YAG laser employed fiber optic beam delivery from a remote laser system to the final delivery optics without any inert gas shielding. The full power of 3 kW was used for the welding process. The energy density/irradiance of the Nd:YAG laser, which is higher than 10^6 W/cm^2, generates a keyhole mode of laser welding [21,22]. Operating speeds were used

Contributed by the Materials Division of ASME for publication in the JOURNAL OF ENGINERING MATERIALS AND TECHNOLOGY. Manuscript received April 3, 2007; final manuscript received October 17, 2007; published online September 9, 2008. Assoc. Editor: Hamid Garmestani.

Table 1 Chemical compositions (%) of the DP980 steel

Steel	C	Si	Mn	Mo	Al	Cr	B	C_{eq} [a]
DP980	0.135	0.05	2.1	0.35	0.45	0.15	0.007	0.51

[a] $C_{eq}=C+A(C)\left(\frac{Mn}{6}+\frac{Si}{24}+\frac{Cr+Mo+V}{5}+\frac{Cu}{15}+\frac{Ni}{20}+\frac{Nb}{5}+5B\right)$ and $A(C)=0.75+0.25\tanh[20(C-0.12)]$.

within the range of 1–6 m/min to obtain full penetration. The welding speed of less than 1 m/min led to the cutting of the material; the speed above 6 m/min led to incomplete penetration.

2.3 Weld Characterization. Weld characteristics were evaluated using both metallographic and microhardness measurements. Metallography was performed using optical microscope and scanning electron microscope (SEM), and microhardness testing was done on weldment transverse sections metallographically mounted, polished, and etched with 2% Nital, using an HMV-2000 testing system with a Vickers indenter at a load of 500 g. Traverses normally used a step distance between indentations of 0.3 mm on diode and 0.15 mm on Nd:YAG laser welds.

Uniaxial tensile testing specimens were of "half size" ASTM E8 dimensions for sheet metal testing. Tensile testing was carried out using an Instron model 4206 universal testing machine, operating at a crosshead speed of 2 mm/min.

Formability tests of the base metal and welded specimens were conducted on a standard limiting dome height (LDH) testing machine, according to ASTM E643–84 standards [13], as shown in Fig. 1. Essentially to have biaxial pure stretching deformation, all LDH test coupons were fully circular, without cutouts. The weld bead was oriented at the center of the 101.6 mm (4 in.) diameter hemispherical punch. Welding was conducted both perpendicular and parallel to the rolling direction. The upper and lower dies had a bead diameter of 254 mm (10 in.). A clamping force of 667 kN was used to secure the test specimens. A punch travel speed of 10 m/min was used. A light coating of mill oil, followed by a 0.05 mm thick plastic sheet, provided the lubrication between the punch face and the blank surface. LDH represents the maximum height to which a sheet specimen could stretch at the onset of fracture.

Table 2 Mechanical properties and chemical composition of the DP980 steel

Steel	Yield strength (MPa)	Ultimate strength (MPa)	Elongation (%)	Hardness (*HV*)	Thickness (mm)
DP980	534	980	12.2	283 ± 2	1.2

Table 3 Laser system characteristics

Laser machine	Laser type	Power (kW)	Focal length (mm)	Beam size (mm)
Nuvonyx ISL-4000L	Diode	4000	80	0.5×12
Haas HL3006D	Nd:YAG	3000	200	0.6

3 Results

3.1 Hardness and Microstructural Analysis. Figure 2 depicts typical hardness profiles of the DP980 steel welded with both lasers. The high welding speed achievable with the Nd:YAG laser led to significantly smaller weld and HAZ width compared with the diode laser. This observation was primarily due to the high irradiance of the Nd:YAG laser resulting in a keyhole mode weld, generating a shorter thermal cycle that led to a shallower, narrower softened zone in the outer HAZ.

The hardness profile was relatively flat across the weld metal itself, showing a very high hardness in the weld metal and high-temperature (inner) HAZ, as could be expected from its chemistry. This region is fully austenized during the laser welding process. A high cooling rate generated in the laser welding process, in combination with high carbon equivalent for the DP980 steel evaluated with Yurioka formula, results in the fully martensitic microstructure in the inner heat affected and fusion zone [24].

In this steel, the hardness showed a progressive decrease moving outward through the HAZ, i.e., with a lower peak temperature experienced in the weld thermal cycle. Hardness "valleys" or softened zones were seen in the outer part of the HAZ (outer HAZ) for all welds where hardness locally dropped significantly below the base metal hardness. This is not the case for the Nd;YAG weld where there is a "small" drop in hardness. Such softened zones had previously been seen in the HAZ of DP steels [2,4,24] and have been attributed to local tempering of the martensite phase of the as-manufactured steel. The cross-sectional views of the weldments of both diode and Nd:YAG are represented in Figs. 3(*a*) and 4(*a*) and the base metal microstructure of the DP steel is repre-

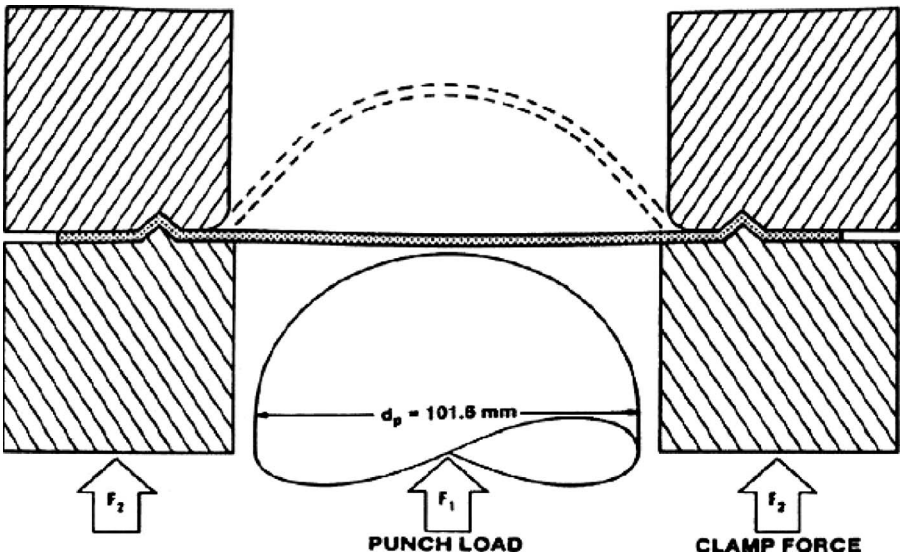

Fig. 1 Schematic representation of the limiting dome height testing [23]

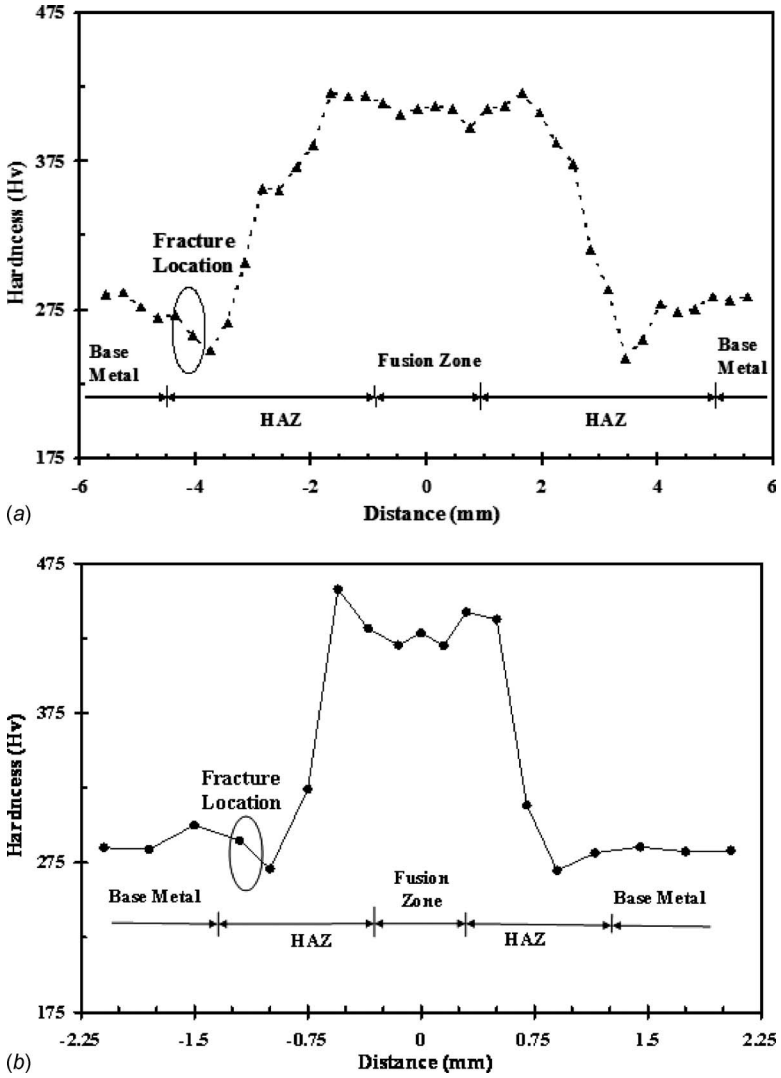

Fig. 2 Typical hardness profile: (*a*) diode at 1 m/min and (*b*) Nd:YAG welds at 3 m/min

sented in Fig. 3(*b*). Microstructural examination also confirmed that the hardness valleys were directly related to tempering: The local decomposition of martensite could be observed, as depicted in Figs. 3(*c*) and 4(*b*). The volume of tempering of martensite is less in Nd:YAG weld due to the keyhole mode of the weld than the conduction mode weld of the diode laser.

The weld metal hardness and microstructure were not strongly affected by welding speed (which affects the shape of the thermal cycle caused by the welding operation). However, the welding speed and the different mode of laser welding (conduction and keyhole) did have a significant effect on the softened HAZ, affecting its location, width, and the minimum hardness. Consistently, with the increase in the welding speed, the width and degree of softening were both reduced, as seen in Fig. 5. The degree of softening is represented by the hardness difference between the base metal and the minimum hardness in the soft zone region.

3.2 Tensile Testing. Figure 6 shows tensile specimens before and after testing, in which gridding of the samples was done to observe the deformation pattern. It was observed from the results that the shape of the grid was changed from circle to oval only at the outer HAZ. Failure occurred by ductile rupture in the outer HAZ within the location of the hardness valley. Examination of the deformation pattern along the specimens showed that yielding occurred first in the softened zone and much of the total plastic strain was concentrated at the outer HAZ.

Figure 7 shows representative engineering stress-strain curves from tensile testing of the base metal and the transverse welded samples. Weldment yield strength and ultimate tensile strength were lower than the base metal values as premature yielding occurred in the softened zone of the outer HAZ. Furthermore, overall specimen elongation was reduced, as necking and failure occurred in the outer HAZ before the rest of the specimen had fully work hardened.

3.3 Formability Testing. Figure 8 shows representative outputs of LDH testing of the base metal and diode welds made parallel and perpendicular to the rolling direction on the DP steel. The LDH of the base metal was 30.4 mm and that of the diode welded sample was 13.1 mm. Formability was drastically reduced up to 57% with respect to the base material in the welded DP steel. The LDH of the welded specimens at fracture was much lower than the corresponding base metal, which indicates that the formability of that material was significantly reduced by the welding process.

In this DP steel, as seen in Fig. 8, the welding direction with respect to the rolling direction of the steel did not significantly influence the formability. The dotted curve represents the formability results of the sample with the welding perpendicular to the rolling direction and the solid curve represents the same with the

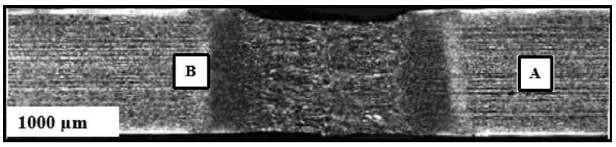

(*a*)

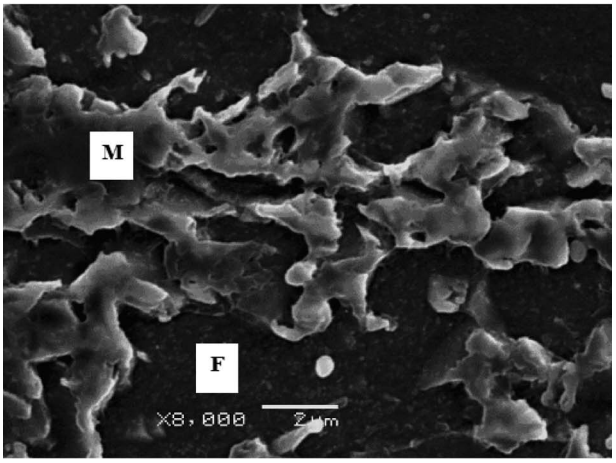

(*b*)

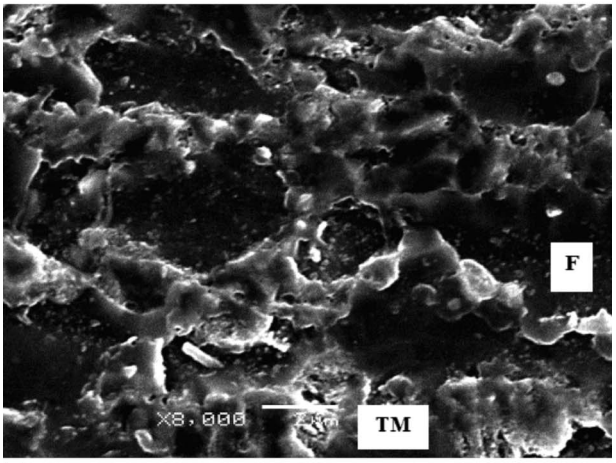

(*c*)

Fig. 3 (*a*) Optical photo; cross section of a Nd:YAG weld at 6 m/min, (*b*) SEM photos of the base metal, and (*c*) tempered zone (M, martensite; F, ferrite; and TM; tempered martensite)

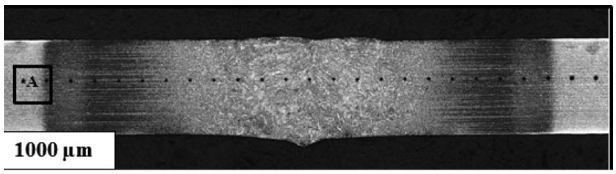

(*a*)

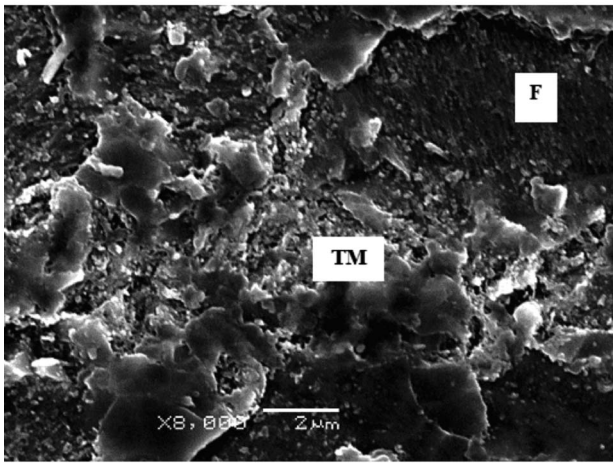

(*b*)

Fig. 4 (*a*) Optical photo; cross section of a diode weld at 0.7 m/min and (*b*) SEM photo of (*a*) tempered zone (M, martensite; F, ferrite; and TM, tempered martensite)

welding parallel to the rolling direction of the steel. Therefore there was no significant difference for the formability of the DP steel with respect to the welding along or perpendicular to the rolling direction, as the behavior of the softened zone dominated the formability.

The influence of the orientation of the weld samples with respect to the dome test equipment was also investigated. Experiments were conducted for each position (the root side and face side) of the weld samples facing the punch. Table 4 represents the LDH results for the diode weld samples for each of the positions. Placing the similar thickness weld sample on the crown/top of the punch of the dome test equipment with the face side or root side of the weld did not significantly change the formability of the DP steel, which is consistent with previous results [8].

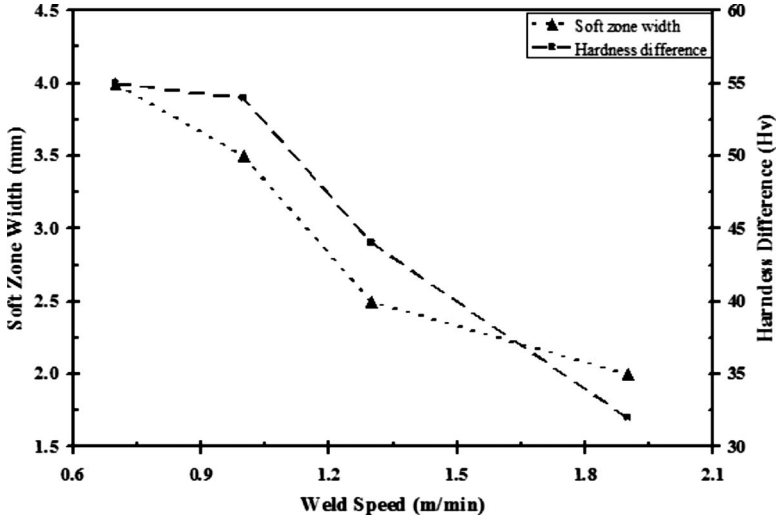

Fig. 5 Relationship between the soft zone width and the degree of softening to various diode laser welding speeds

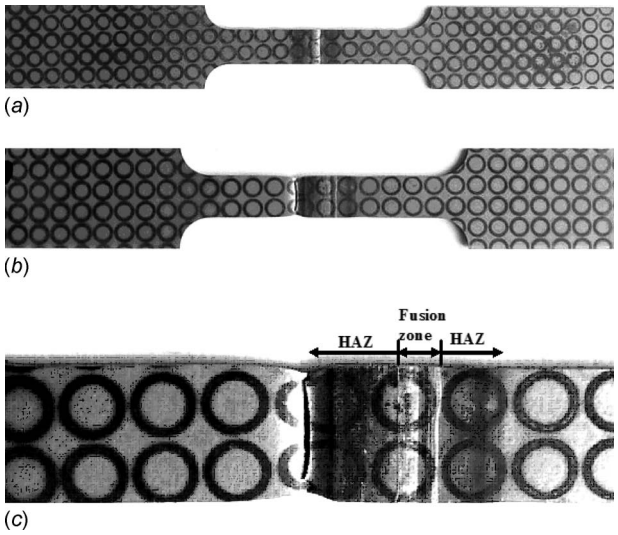

Fig. 6 Tensile test specimen of the diode weld at 1.45 m/min: (*a*) before test, (*b*) after test, and (*c*) close up view of the necking and fracture region

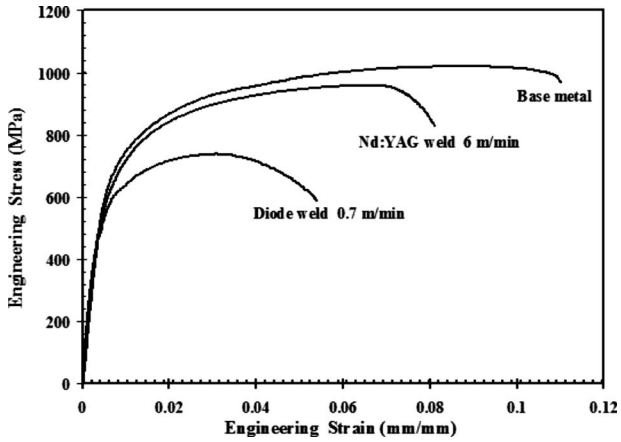

Fig. 7 Representative results of engineering stress versus engineering strain of the uniaxial tensile tests

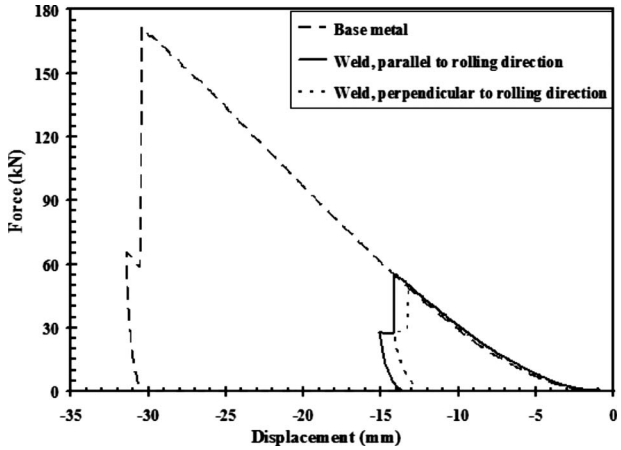

Fig. 8 Typical limiting dome height results of the base metal and diode welded specimens at 1.6 m/min welding speed

Table 4 Diode laser weld orientation on the punch of the formability equipment at 2 m/min

Orientation	LDH (mm)
Face side	11.03
Root side	11.14

Figure 9 depicts the relation between formability ratio and welding speed for welds with both lasers. The formability ratio is given in Eq. (1):

$$\text{formability ratio} = \text{LDH of welded sample/LDH of base metal} \quad (1)$$

Formability was higher for higher welding speed, as an increase in welding speed led to reduced specific energy input and faster cooling after passage of the laser beam. This resulted in a smaller softened zone created in the specimen. For the same weld parameter, Nd:YAG welds had better formability, which may be due to the fact that they have smaller softened zone due to the keyhole mode of welding than the welds made with the low irradiance diode laser that operate in the conduction mode welding, generating a longer thermal cycle that led to a deeper, broader softened zone in the outer HAZ, as seen in Fig. 2.

Top views of the tested specimens, i.e., the base metal and welds made using two types of lasers, until the point of fracture in the specimen, are shown in Fig. 10. In the base metal, the fracture path was at a radial distance of about 17 mm from the disk center and propagated in a direction parallel to the rolling directions in all tests, as seen in Fig. 10. This DP steel therefore displayed significant directionality in terms of formability. In diode and Nd:YAG laser weldments, the fracture path was always entirely in the outer HAZ, regardless of the welding speed and whether the welding direction was parallel or perpendicular to the rolling direction, suggesting severe strain concentration in that zone. The formability tests showed consistent behavior and similar fracture locations to the tensile tests.

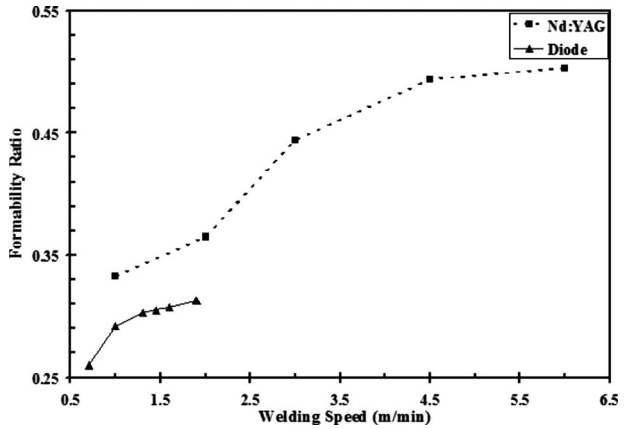

Fig. 9 Relation between formability ratio and welding speed for welds with both lasers

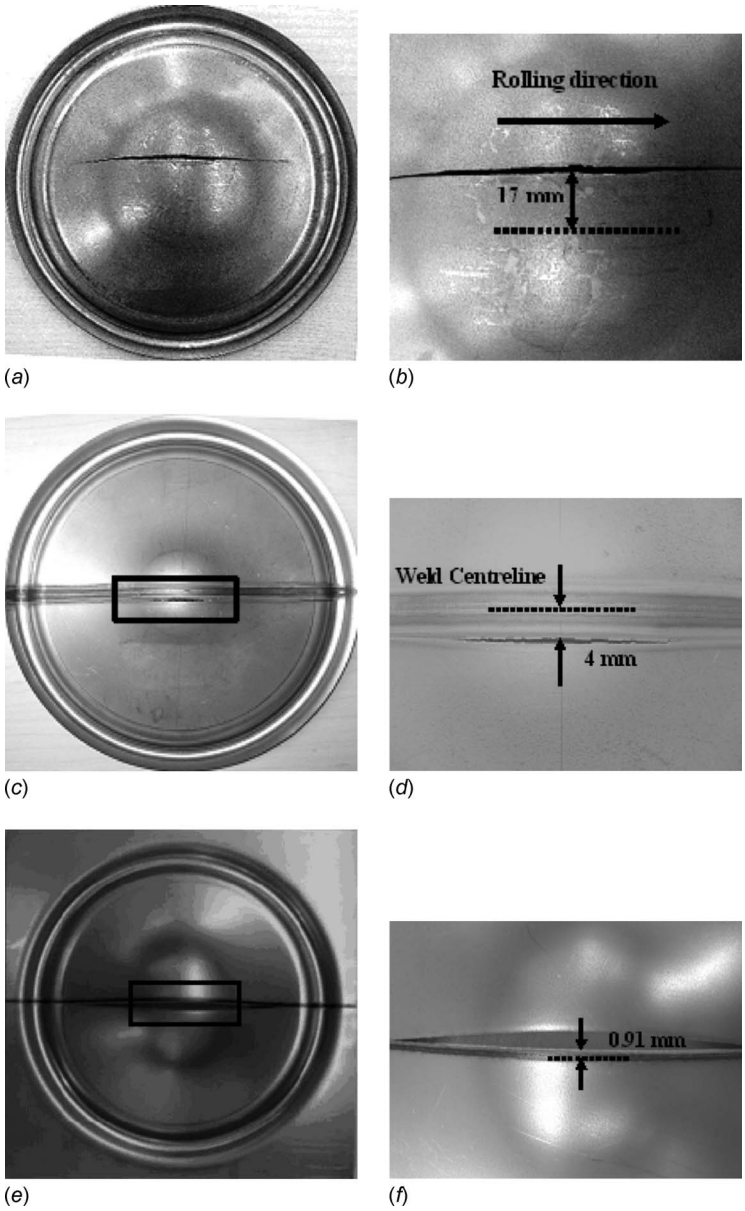

Fig. 10 Top view of the dome tested specimens: (*a*) base metal, (*b*) closer view of the fracture, (*c*) diode welded specimen at 1.3 m/min, (*d*) closer view of the fracture in (*c*), (*e*) Nd:YAG welded specimen at 6.0 m/min, and (*f*) closer view of the fracture in (*e*)

Figure 11 shows relationships between the welding speed and fracture and softened zone distances from the weld centerline in the biaxial test (LDH). Fracture distances from the weld centerline in both the uniaxial and biaxial tests were similar. The fracture and softened zone distances from the weld centerline were inversely related to the welding speed. Higher welding speed is expected to generate faster cooling rates, which will generate the same peak temperatures in the HAZ at a smaller distance from the weld center. In welds with both lasers, fracture occurred slightly farther out from the weld centerline than the softest zone. It appeared that the hardened inner HAZ and the fusion zone restricted the deformation and pushed the failure a little farther out from the softest zone. The fracture distance from the weld center was higher for the diode laser weld than for the Nd:YAG laser weld at the same welding speed. Diode and Nd:YAG lasers have different power densities generating conduction and keyhole mode laser welding, respectively, which evidently develop a different welding thermal cycle for the same welding speed [21], i.e., less irradiance in diode laser resulted in a softened zone farther away from the weld center.

4 Discussion

In this section, the effects of softened zone characteristics and base metal elongation of the welded DP steel on formability are discussed. Furthermore, the relationship between the uniaxial and biaxial strains is also considered.

Figure 12 represents the relationship between the formability (LDH) and the reduction in hardness. The reduction in hardness is represented in Eq. (2):

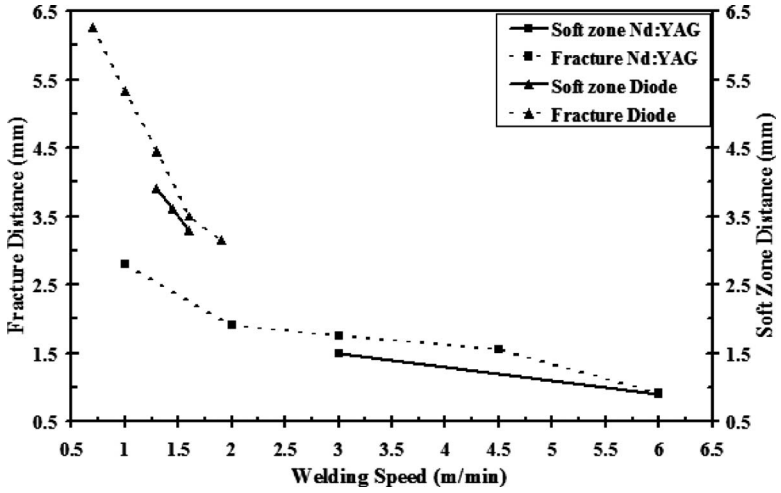

Fig. 11 Softened zone and fracture distance from the weld center for welds with both lasers

$$\text{reduction in hardness } (\%) = (HV_{bm} - HV_{sz})/HV_{bm} \times 100 \quad (2)$$

where HV_{bm} is the hardness of the base metal and HV_{sz} is the minimum hardness of the softened zone.

It was observed from the plot that larger reductions in hardness led to lower formability of the welded blanks. Different curve fitting operations were attempted to obtain the best fit for the experimental results, in which an exponential curve (shown in Fig. 12) fitted the data well with the coefficient of determination (R value) of 98%.

The formability of the diode welds was less than that of the Nd:YAG welds, as the softened zone in the diode welds is larger than that of the Nd:YAG welds, as shown in Fig. 12. With an increase in the welding speed, the formability of the welded DP steel samples approaches that of the base metal. These results indicate that for higher power density and hence higher speed keyhole mode there is a smaller softened zone; therefore, for the DP steel it is better to weld with the Nd:YAG laser in the keyhole mode and at the maximum achievable welding speed.

Butt weld joint performance in transverse tensile testing using finite element analysis (FEA) combined with design of experiments (DOE) has been studied by other researchers [25], who also discussed the influences of geometry and material properties on the transverse tensile tests. It was found through detailed FEA study that HAZ hardness was an important factor in the transverse tensile performance. The hardness traverses across the weldment were a good indicator of the formability of the material [19]. One of the simulation cases had HAZ hardness less than either base metal or weld metal hardness (HAZ $HV <$ base metal $HV <$ weld metal HV), which is similar to the experimental results of this work. Interestingly, fracture initiation and failure were in the HAZ, which coincides with this work. The resulting tensile strength and the displacement were the lowest among all cases discussed in their studies. Their results validate the observation that the reduction in hardness was an important influence on transverse tensile tests, which is closely related to the reduction in formability.

Two steels of the same grade (DP980) with different base metal

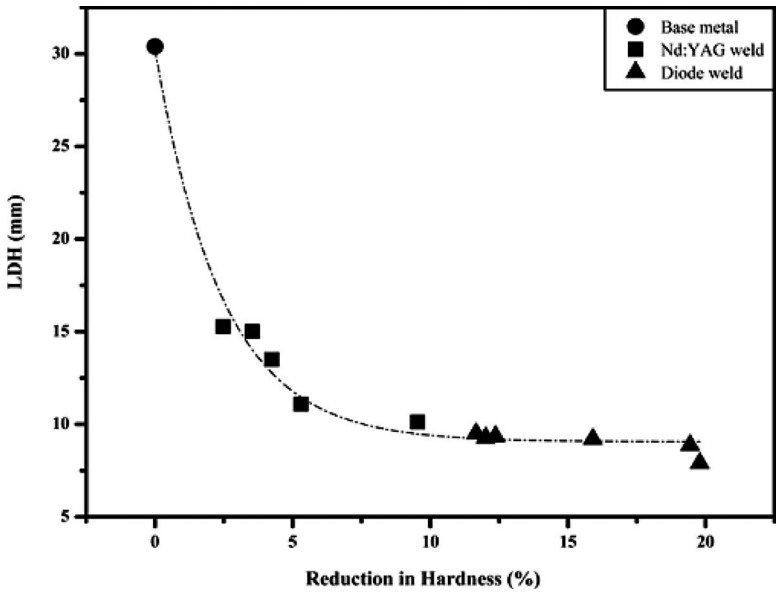

Fig. 12 Relationship between reduction in hardness and limiting dome height

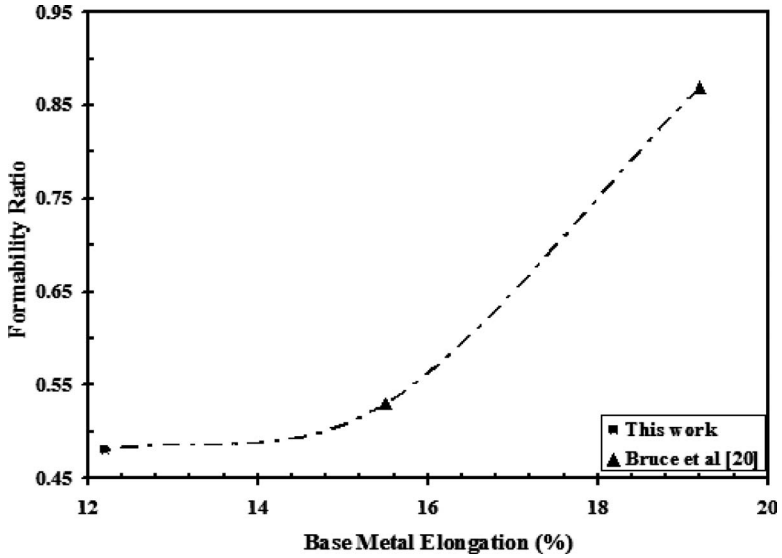

Fig. 13 Relationship between formability ratio and base metal elongation of the same grade of steel with laser weld of same welding parameters (3 kW, 4 m/min)

elongation and welded with the same welding parameters (3 kW, 4 m/min) were used for formability tests by Bruce and Moraki [18]. It was observed from their work [18] that the formability of the laser welded high strength DP steel was higher when the base material elongation was higher. This result confirms the conclusion of Uchihara and Fukui [5]. Furthermore, to investigate the formability of the same grade of the DP steel with the same welding parameters, test welds were conducted in the present study. The base metal elongation of the DP steel used in this work was smaller than that of the two DP steels described in Ref. [18]. Figure 13 depicts the relation between the formability ratio as defined in Eq. (1) and the base metal elongation of the welded DP steels in the present work as compared with that of Bruce and Moraki [18].

This result validates the effect of the base metal elongation on the formability of the welded DP steel. The higher base metal elongation means higher strain hardening exponent (n-value) of the base metal. The n-value describes the material's ability to uniformly distribute deformation or elongation. The material of higher n-value will have greater uniform elongation in the presence of local strength variations and will also resist localized deformation or necking.

This result shows a good and predictable relationship of the formability with the base metal elongation of the laser welded joint. DP steels with higher base metal elongation are preferred for the formability aspect of the laser welded specimen.

Figure 14 represents the relationship between the uniaxial and the biaxial strain of the base metal and diode welded samples of the DP980 material. The average measured strain in tensile tests and the average measured strain in LDH tests appeared to have a stable and predictable relationship.

The measured biaxial strain was higher than the uniaxial strain in the base metal specimen. This is consistent with the behavior expected from the forming limit diagram (FLD) [26]. However, the measured biaxial strain was less than the uniaxial strain in welded specimens. The ratio of the softened zone size (width) to the gauge length of the LDH specimens was smaller than the ratio of the softened zone size to the gauge length of the uniaxial tensile

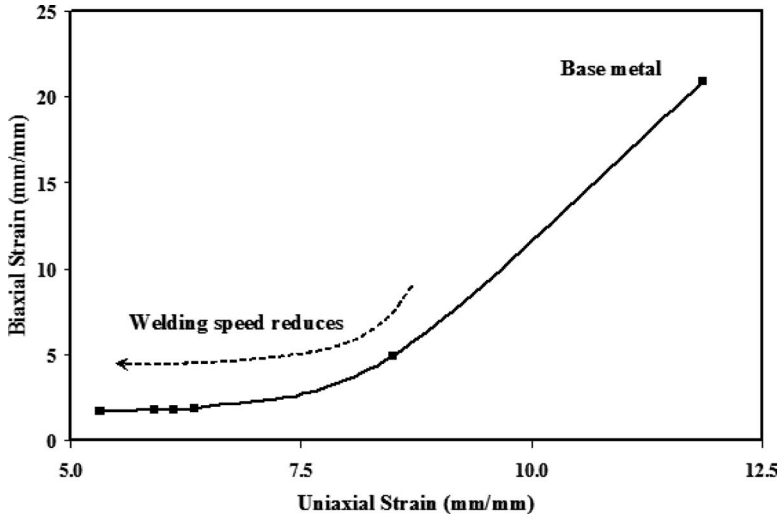

Fig. 14 Relationship between biaxial and uniaxial strains and weld speed

test specimens. Hence the localized strain concentration developed in the biaxial test will be smaller compared with the uniaxial tensile test.

The results showed that fracture and failure in both the uniaxial tensile test and the biaxial LDH test were in the outer HAZ of the laser welded DP steel, indicating that the transverse tensile testing is a useful indicator for the formability of the welded DP steel.

5 Conclusions

In the DP980 steel used in this work, all diode and Nd:YAG laser weld parameters studied, from high to low speeds, generated a softened zone in the outer heat affected zone.

Dimensions (depth and width) of the softened zone were found to be inversely related to welding speed and to the irradiance of the laser.

Formability was significantly affected by the presence of the softened zone in this welded steel, with a reduction in formability becoming greater as the softened zone size increased.

The higher welding speed was achieved as the irradiance of the Nd:YAG laser develops a keyhole mode of welding, which generated a shorter weld thermal cycle and hence a smaller softened zone, yielding a better formability of welded blanks.

No significant difference was observed in the formability of the DP980 steel with change in the welding orientation relative to the rolling direction or variation of the welded specimen location on the punch (face or root side of the weld), as softened zone dominated the formability behavior.

Both in uniaxial tensile test and biaxial LDH test, the fracture occurred in the softened zone of the welded samples consistently slightly farther out from the weld centerline than the location of the minimum hardness.

References

[1] Ghosh, P. K., Gupta, P. C., Avtar, R., and Jha, B. K., 1990, "Resistance Spot Weldability of Comparatively Thick C-Mn-Cr-Mo Dual Phase Steel Sheet," ISIJ Int., **30**(3), pp. 233–240.

[2] Ghosh, P. K., Gupta, P. C., Avtar, R., and Jha, B. K., 1991, "Weldability of Intercritical Annealed Dual-Phase Steel With the Resistance Spot Welding Process," Weld. J. (Miami, FL, U.S.), **70**(1), pp. 7s–14s.

[3] Larsson, K. J., 2002, "Supporting Welding Methods for Future Light Weight Steel Car Body Structures," SAE Technical Paper Series No. 2002-01-2091.

[4] Schaik, M., and Wenk, D., 2003, "The Future for Welding of AHSS Tailored Blanks," SAE Technical Paper Series No. 2003-01-2779.

[5] Uchihara, M., and Fukui, K., 2003, "Tailored Blanks of High Strength Steels—Comparison of Welding Processes," SAE Technical Paper Series No. 2003-01-2829.

[6] Ramasamy, S., and Albright, C. E., 2000, "CO_2 and ND:YAG Laser Beam Welding of 6111-T4 Aluminum Alloy for Automotive Applications," J. Laser Appl., **12**(3), pp. 101–110.

[7] Ghoo, B. Y., and Kim, Y. S., 2001, "Evaluation of the Mechanical Properties of Welded Metal in Tailored Steel Sheet Welded by CO_2 Laser," J. Mater. Process. Technol., **113**, pp. 692–698.

[8] Scriven, P. J., Brandon, J. A., and Williams, N. T., 1996, "Influence of Weld Orientation on Forming Limit Diagrams of Similar/Dissimilar Thickness Laser Welded Joints," Ironmaking Steelmaking, **23**(2), pp. 177–182.

[9] Howard, K., Lawson, S., and Zhou, Y., 2006, "Welding Aluminum Sheet Using a High-Power Diode Laser," Weld. J. (Miami, FL, U.S.). **85**(5), pp. 101s–110s

[10] Abe, N., Tsukamoto, M., Morikawa, A., Maeda, K., and Namba, K., 2002, "Welding of Aluminum Alloy With High Power Direct Diode Laser," Trans. JWRI, **31**(2) pp. 157–163.

[11] Herfurth, H. J., and Ehlers, B., 2000, "Increased Performance Broadens Processing Capabilities of High Power Diode Lasers," *Proceedings of the ICALEO, Laser Applications in the Automotive Industry*, Dearborn, MI, May 9–12, Vol. 91, pp. D9–D18.

[12] Chan, L. C., Chan, S. M., Cheng, C. H., and Lee, T. C., 2005, "Formability Analysis of Tailor-Welded Blanks of Different Welded Blanks of Different Thickness," ASME J. Eng. Mater. Technol., **127**, pp. 743–751.

[13] Breakiron, B., and Fekete, J. R., 2005, "Formability Analysis of High-Strength Steel Laser-Welded Blanks," SAE Technical Paper Series No. 2005-01-1326.

[14] Saunders, F. I., and Wagoner, R. H., 1996, "Forming of Tailor-Welded Blanks," Metall. Mater. Trans. A, **27**, pp. 2605–2616.

[15] Waddell, W., Jackson, S., and Wallach, E. R., 1998, "The Influence of the Weld Structure on the Formability of Laser Welded Tailored Blanks," Metall. Mater. Trans. A, **27**, pp. 257–268.

[16] Dry, D., Hughes, D., and Owen, R., 2001, "Methods of Assessing Influence of Weld Properties on Formability of Laser Welded Tailored Blanks," Ironmaking Steelmaking **28**(2), pp. 89–95.

[17] Lawson, S., Li, X., and Zhou, Y., 2006, "Investigation of Laser Weldability of Some Advanced High Strength Sheet Steels," *Proceedings of the Sheet Metal Welding Conference XII*, Livonia, MI, May 9–12.

[18] Bruce, H., and Moraki, O., 2002, "Laser Weldability of Dual Steels in Tailored Blank Applications," SAE Technical Papers Series No. 2002-01-0150.

[19] Xia, M., Sreenivasan, N., Lawson, S., and Zhou, Y., 2007, "A Comparative Study of Formability of Diode Laser Weldments in DP980 and HSLA Steels," ASME J. Eng. Mater. Technol., **129**(3), pp. 446–452.

[20] Yurioka, N., Suzuki, H., Ohshita, S., and Saito, S., 1980, "Determination of Necessary Preheating Temperature in Steel Welding," Weld. J. (Miami, FL, U.S.), **62**, pp. 147s–153s.

[21] Duley, W. W., 1999, *Laser Welding*, Wiley, New York.

[22] Ready, J. F., and Farson, D. F., 2001, *LIA Handbook of Laser Materials Processing*, Laser Institute of America.

[23] Anand, D., 2004, "Formability and Fatigue Behavior of Tailor (Laser) Welded Blanks for Automotive Applications," MS thesis, Ryerson University, Toronto.

[24] Biro, E., and Lee, A., 2004, "Welding Properties of Various DP600 Chemistries," *Proceedings of the Sheet Metal Welding Conference*, Sterling Heights, MI, May 11–14.

[25] Martilla, W. A., and Forrest, M. G., 2006, "FEA Study of Butt Joint Tensile Performance in Support of Filler Wire Selection for Arc Welding Advanced High-Strength Steels," International Institute of Welding Conference, Quebec City, Canada, Aug. 29, Paper No. III-1389-06.

[26] Keeler, S., and Brazier, W. G., 1975, "Relationship Between Laboratory Material Properties and Press Shop Formability," *Proceedings of Conference on Microalloy 1975*, New York, pp. 517–527.